NUCLEOSYNTHESIS

Element abundance patterns in stars indicate fission of nuclei heavier than uranium

Ian U. Roederer[1]*†, Nicole Vassh[2], Erika M. Holmbeck[3], Matthew R. Mumpower[4,5], Rebecca Surman[6], John J. Cowan[7], Timothy C. Beers[6], Rana Ezzeddine[8], Anna Frebel[9,10], Terese T. Hansen[11], Vinicius M. Placco[12], Charli M. Sakari[13]

The heaviest chemical elements are naturally produced by the rapid neutron-capture process (*r*-process) during neutron star mergers or supernovae. The *r*-process production of elements heavier than uranium (transuranic nuclei) is poorly understood and inaccessible to experiments so must be extrapolated by using nucleosynthesis models. We examined element abundances in a sample of stars that are enhanced in *r*-process elements. The abundances of elements ruthenium, rhodium, palladium, and silver (atomic numbers Z = 44 to 47; mass numbers A = 99 to 110) correlate with those of heavier elements ($63 \leq Z \leq 78$, $A > 150$). There is no correlation for neighboring elements ($34 \leq Z \leq 42$ and $48 \leq Z \leq 62$). We interpret this as evidence that fission fragments of transuranic nuclei contribute to the abundances. Our results indicate that neutron-rich nuclei with mass numbers >260 are produced in *r*-process events.

The heaviest chemical elements are synthesized through the rapid neutron capture process (*r*-process). Sites where the *r*-process occurs include mergers of neutron stars, which have been observed (*1*–*3*). The nuclei produced by the *r*-process in these events depend on the composition of material ejected by the merger (*4*) and the properties of the progenitor neutron stars, including their equation of state (*5*). Freshly produced lanthanide elements (atomic numbers Z = 57 to 71) (*6*, *7*) and Sr (Z = 38) (*8*) have been observed in the ejecta of a neutron star merger event, but otherwise the detailed chemical composition has not been measured.

The detailed compositions of some ancient stars in the Milky Way have been determined from their spectra, which contain hundreds of absorption features of more t 40 *r*-process elements (*9*). The abund patterns of lanthanide elements in these stars are nearly identical, indicating a possible universality of *r*-process events and producing the same abundance ratios. The composition of each star is dominated by the ejecta of individual *r*-process events (*10*, *11*), such as neutron star mergers or rare types of supernova,

[1]Department of Astronomy, University of Michigan, Ann Arbor, MI 48109, USA. [2]TRIUMF (Tri-University Meson Facility), Vancouver, BC V6T 2A3, Canada. [3]Carnegie Observatories, Pasadena, CA 91101, USA. [4]Theoretical Division, Los Alamos National Laboratory, Los Alamos, NM 87545, USA. [5]Center for Theoretical Astrophysics, Los Alamos National Laboratory, Los Alamos, NM 87545, USA. [6]Department of Physics and Astronomy, University of Notre Dame, Notre Dame, IN 46556, USA. [7]Homer L. Dodge Department of Physics and Astronomy, University of Oklahoma, Norman, OK 73019, USA. [8]Department of Astronomy, University of Florida, Bryant Space Science Center, Gainesville, FL 32611, USA. [9]Department of Physics, Massachusetts Institute of Technology, Cambridge, MA 02139, USA. [10]Kavli Institute for Astrophysics and Space Research, Massachusetts Institute of Technology, Cambridge, MA 02139, USA. [11]Department of Astronomy, Stockholm University, AlbaNova University Center, SE-106 91 Stockholm, Sweden. [12]National Optical-Infrared Astronomy Research Laboratory, National Science Foundation, Tucson, AZ 85719, USA. [13]Department of Physics and Astronomy, San Francisco State University, San Francisco, CA 94132, USA.
*Corresponding author. Email: iuroederer@ncsu.edu
†Present address: Department of Physics, North Carolina State University, Raleigh, NC 27695, USA.

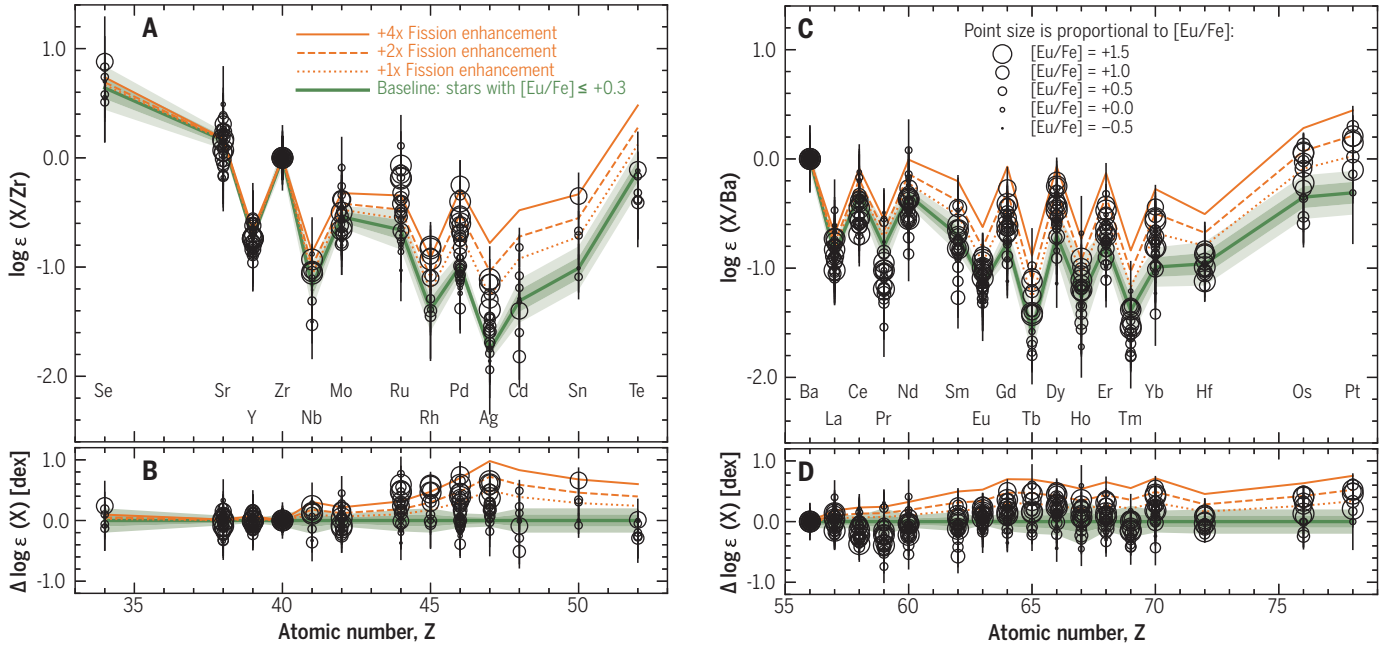

Fig. 1. Observed abundance patterns compared with fission model predictions. Shown are logarithmic abundances (open circles) measured for 30 *r*-process elements in the 42 stars of our sample, plotted as a function of atomic number. The symbol sizes are proportional to [Eu/Fe], and error bars indicate 1σ uncertainties. The green line is the empirical baseline pattern we defined as the mean abundance ratios for the subset of 13 stars with [Eu/Fe] ≤ +0.3. Light shading and dark green shading indicate ± 1 and ± 2 times the standard error in the baseline, respectively. The orange lines indicate models of fission fragments added to the baseline pattern; the dotted line has equal contributions from the baseline and the fission model, the dashed line has two parts fission fragments plus one part baseline pattern, and the solid line has four parts fission plus one part baseline. (**A**) Elements $34 < Z < 52$, normalized to Zr (solid circle). Elements are labeled at bottom. (**B**) Residuals between the data and the baseline pattern in (A). (**C** and **D**) Same as (A) and (B), respectively, but for elements $56 < Z < 78$, normalized to Ba (solid circle). Numerical values are provided in data S1.

which enriched the gas from which the stars formed (*12*).

Stellar sample and abundance measurements

We investigated the *r*-process using a sample of 42 stars in the Milky Way. We selected stars that were previously observed to have heavy elements known to be formed by the *r*-process, with no evidence of contamination from other processes [such as the slow neutron capture process (*s*-process)]. We adopted the element abundances of 31 heavy elements ($34 \leq Z \leq 90$) from data reported in 35 previous studies (*13*) then homogenized these abundances to a common scale using the atomic data reported in the original studies (*13*).

The ratio [Fe/H] is defined as $[\mathrm{Fe/H}] \equiv \log_{10}(N_{\mathrm{Fe}}) - \log_{10}(N_{\mathrm{Fe}})_{\odot}$, where N is the number density with subscript indicating the element, and $\odot$ indicates the value for the Sun. We use Fe as a measure of the overall enrichment by elements heavier than He (referred to as the metallicity). We use the ratio $[\mathrm{Eu/Fe}] \equiv \log_{10}(N_{\mathrm{Eu}}/N_{\mathrm{Fe}}) - \log_{10}(N_{\mathrm{Eu}}/N_{\mathrm{Fe}})_{\odot}$ as a measure of the enhancement of *r*-process elements relative to the metallicity. Our sample spans the ranges $-3.57 \leq [\mathrm{Fe/H}] \leq -0.99$ and $-0.52 \leq [\mathrm{Eu/Fe}] \leq +1.69$ (data S1).

Correlations between elements

The heavy-element abundance patterns in the selected stars are shown in Fig. 1 (individual elements are shown in figs. S3 and S4). We found that stars with higher [Eu/Fe] ratios have abundances of some elements (including Ru, Rh, Pd, Ag, Gd, Tb, Dy, and Yb) that are slightly enhanced relative to those in stars with lower [Eu/Fe] ratios. This excess is not an expected consequence of *r*-process universality.

We calculated an empirical baseline abundance pattern (tables S2 and S3) using the 13 stars (30% of the sample) with the lowest levels of *r*-process enhancement, $[\mathrm{Eu/Fe}] \leq +0.3$. The abundance excess—the difference between the individual abundance measurements in each star and the empirical baseline for that element—is shown for all stars in Fig. 1, B and D, and split into different groups of elements in Fig. 2. Three sets of elements behave similarly in our sample: Se, Sr, Y, Zr, Nb, and Mo ($34 \leq Z \leq 42$); Cd, Sn, and Te ($48 \leq Z \leq 52$); and Ba, La, Ce, Pr, Nd, and Sm ($56 \leq Z \leq 62$), shown in Fig. 2, A, C, and D, respectively. The abundance ratios of these elements exhibit no

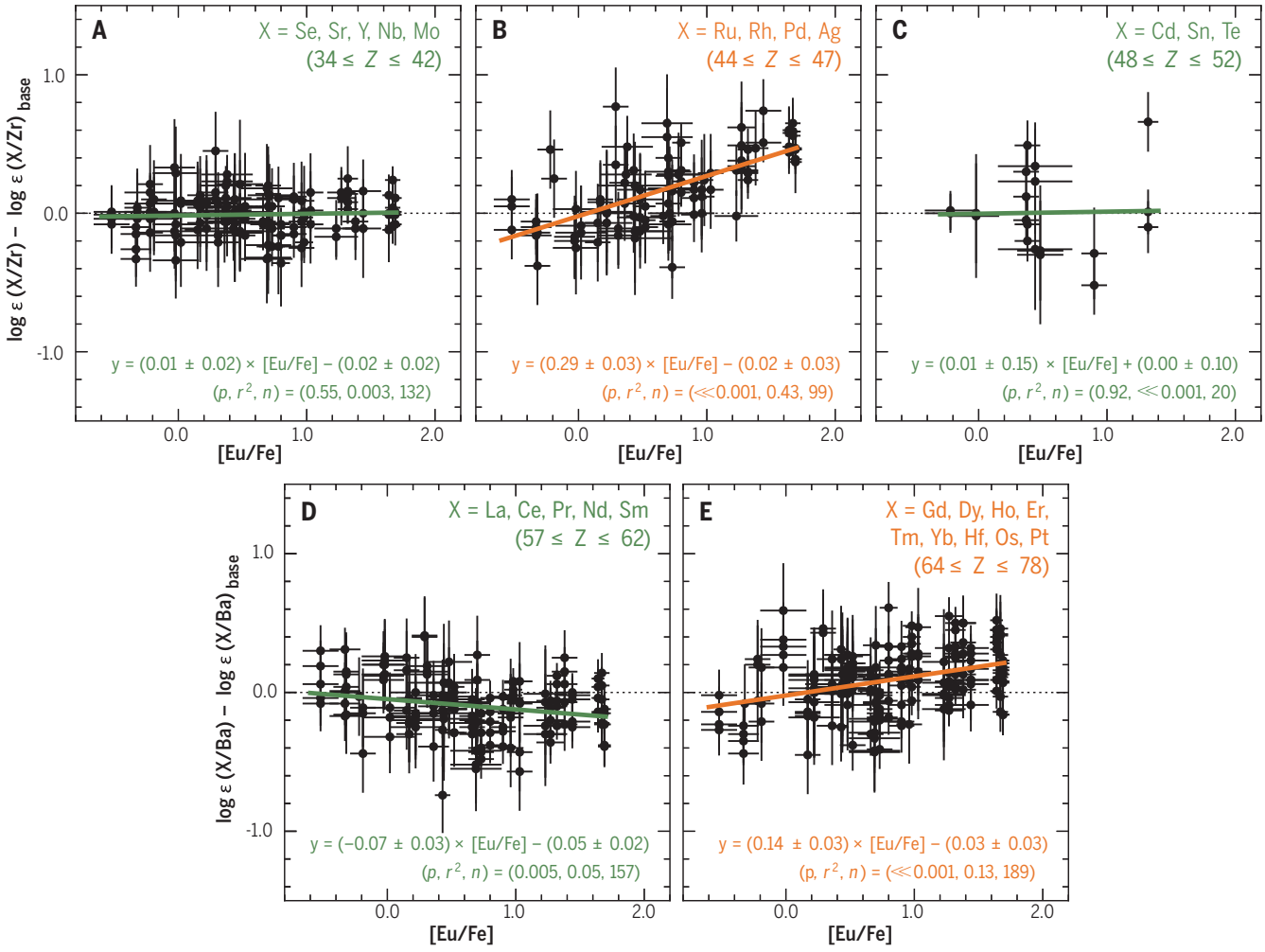

Fig. 2. Abundance ratios of groups of elements that do or do not correlate with [Eu/Fe]. (**A** to **E**) Different groups of elements, ordered by increasing atomic number *Z*. (A) $34 \leq Z \leq 42$. (B) $44 \leq Z \leq 47$. (C) $48 \leq Z \leq 52$. (D) $57 \leq Z \leq 62$. (E) $64 \leq Z \leq 78$. In (A) to (E), black data points are for one element abundance ratio in one star, with the error bars indicating 1σ uncertainties. Abundances have been normalized to Zr in (A) to (C) and Ba in (D) and (E), and the empirical baselines shown in Fig. 1 have been subtracted. Solid lines indicate ordinary least-squares linear fits to the data, and dotted lines indicate differences of zero. Green indicates flat trends (lines consistent with zero); we interpret these as indicating that those elements are produced together with Zr or Ba. Orange indicates correlations that are significantly (>4.6σ) different from zero; we interpret these as indicating those elements are produced together with Eu. Labels indicate the equation of each fitted line, the *P*-value of its Pearson correlation coefficient; the coefficient of determination, r^2; and the number of stars, *n* (*13*); these values are also listed in table S1. Separate plots for each element are shown in figs. S3 to S5.

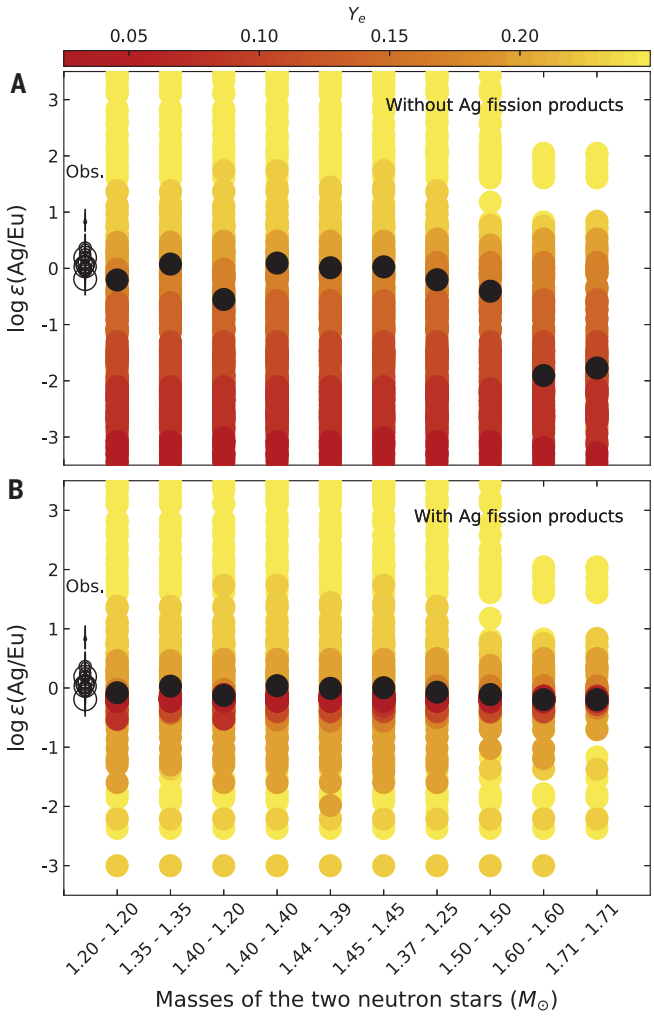

Fig. 3. Ag/Eu abundance ratios predicted with nucleosynthesis models. Predictions of log ε(Ag/Eu) from hydrodynamic simulations (*13*) of neutron star mergers are plotted as a function of the pair of progenitor masses. Overlapping colored dots indicate individual ejecta, and black dots indicate the mean mass-weighted abundance ratio (*13*). The color bar indicates the neutron richness (Y_e) of individual ejecta; lower Y_e ejecta are expected to experience more fission. Open circles indicate the observed ratios in our stellar sample, with sizes proportional to the [Eu/Fe] ratio in each star (as in Fig. 1). Results are shown for models (**A**) without including fission and (**B**) with fission included. When fission is included, we found that the predicted mass-weighted log ε(Ag/Eu) ratios are independent of the progenitor masses and are consistent with the observations.

correlation with [Eu/Fe] and therefore no excess (*13*).

Two other sets of elements exhibit significant (at least 4.6σ) positive correlations with [Eu/Fe] (*13*). These two sets include the elements Ru, Rh, Pd, and Ag ($44 \le Z \le 47$) and Gd, Tb, Dy, Ho, Er, Tm, Yb, Hf, Os, and Pt ($64 \le Z \le 78$), shown in Fig. 2, B and E, respectively. These correlations indicate an extension of *r*-process universality, so that many of the heavier *r*-process elements have abundances linked to those of a smaller number of lighter elements.

Interpretation as fission fragmentation

Two deviations from *r*-process universality have previously been identified (supplementary text). One consists of large differences [>1.5 decimal exponent (dex)] in the overall abundances of light *r*-process elements ($34 \le Z < 56$) relative to heavier ones ($Z \ge 56$) for some elements outside our range of interest ($44 \le Z \le 47$). The other deviation, known as the actinide boost, is characterized by small variations (<0.7 dex) in the abundances of the actinide elements Th ($Z = 90$) and U ($Z = 92$) relative to other heavy *r*-process elements. Neither of these deviations from *r*-process universality can explain the correlations in Fig. 2.

Our findings are also inconsistent with two-component models of *r*-process nucleosynthesis (*14*, *15*), in which one component (referred to as the weak, or limited, *r*-process) dominates the lighter *r*-process elements, and another (referred to as the main *r*-process) dominates the heavier *r*-process elements. Those two-component models segregate light- and heavy-element production so cannot produce abundance correlations between [Eu/Fe] and some, but not all, light *r*-process elements.

We propose that these element groups ($44 \le Z \le 47$ and $63 \le Z \le 78$) were instead produced as fission fragments of transuranic ($Z > 92$) elements that were synthesized in the *r*-process but have since decayed. Nucleosynthesis models have predicted that transuranic elements can be produced in *r*-process events if the ejecta contain very neutron-rich material (*16*–*18*). In this scenario, the synthesis of heavy elements terminates at some maximum mass, above which transuranic nuclei undergo fission and increase the abundances of *r*-process elements at lower masses (*19*).

Fission fragments would reduce any variations in the initial abundances of *r*-process seed nuclei. Natural variations in conditions at nucleosynthesis sites would produce variations in the abundances, but fission fragment deposition could overcome those variations (*20*), leading to fixed relative abundances between the fission products (such as Ag and Eu). Fixed abundance ratios have previously been proposed as a potential signature of fission, according to theoretical calculations and a smaller sample of stars (*21*). Shown in Fig. 3 are theoretical models of neutron star merger dynamical ejecta (*13*), which produce similar log ε(Ag/Eu) ratios [defined as $\log_{10}(N_{Ag}/N_{Eu})$] when fission is included. Models that do not include a fission component near $A = 110$ (Fig. 3A) are sensitive to differences in initial conditions, such as neutron star mass, so predict variable log ε(Ag/Eu) ratios in the ejecta. We refer specifically to fission products near $A = 110$, because all these models include some level of fission in their calculations.

After a neutron star merger event, an accretion disk can temporarily form around the remnant object. Material ejected from this disk is expected to contain few or no nuclei that undergo fission (*22*), so additional ejecta from the disk could produce even larger variations between events. The neutron richness and relative amounts of ejecta from different parts of a neutron star merger event are not well constrained, so there is an unknown contribution of *r*-process synthesis in the disk to elements beyond Sr ($Z = 38$), such as Ag and Pd. We used previous dynamical ejecta simulations (*23*) to investigate the predictions of models that include a fission component for the mass-weighted log ε(Ag/Eu) ratios. We found that they are approximately constant when fission is included (Fig. 3B), which is consistent with the observed stellar ratios. We expect similar results for models of other potential *r*-process sites. For example, the predicted neutron richness of the ejecta of supernovae produced by magnetized and rapidly rotating stars (magneto-rotational supernovae) depends on the strength of the magnetic field (*24*). If fission occurs in any *r*-process site, it acts to reduce the variation in abundance ratios.

We show in Fig. 1 the baseline abundance pattern calculated above, which we assume contains minimal contributions from fission. To illustrate different fission contributions, we also show in Fig. 1 abundance patterns with additional transuranic fission fragments enhanced by factors of 1, 2, and 4 times the baseline (*13*). These enhancement factors were chosen to span the range of abundance excesses we found for elements with $44 \le Z \le 47$ and $63 \le Z \le 78$ in the stars with the highest levels of

[Eu/Fe]. We found that fission fragmentation could explain the elements with the largest observed excesses, including Pd, Ag, Gd, and Yb (*13*). We estimate that up to half of stars known to have $-3.0 \leq$ [Fe/H] ≤ -1.5 could have contributions from fission fragments (*13*). Because the stars in our sample are old, this rate of fission-affected abundances is a property of the dominant *r*-process site in the early Universe.

We conclude that fission fragments of transuranic nuclei can explain the correlations we found between elements with $44 \leq Z \leq 47$ and $63 \leq Z \leq 78$. We investigated whether the observed behavior could be reproduced by other known nucleosynthesis processes—including the weak or main *s*-process, intermediate neutron-capture process, or weak *r*-process—but found that it cannot (supplementary text). Nor can it be explained by the actinide-boost phenomenon, which has previously been observed in some *r*-process–enhanced stars (supplementary text and fig. S6).

Many of the radioactive, neutron-rich nuclei produced during the *r*-process are inaccessible to laboratory experiments, so theoretical models are necessary to estimate their properties by extrapolating from more stable isotopes. Models predict that many of these nuclei have asymmetric fission fragment distributions, with a lighter peak and a heavier peak (*13*, *25*). We propose that the lighter fragments likely contribute to the Ru, Rh, Pd, and Ag abundances in our dataset. Neutron-rich nuclei with mass numbers $99 \leq A \leq 110$, produced directly through fission, are expected to experience β decay until they become the observed elements (*26*). If we assume that the heavier fragments contribute to the Eu and heavier elements ($A > 150$) in our sample, then nuclei with $A > 260$ (110 + 150) were produced in the *r*-process.

REFERENCES AND NOTES

1. B. P. Abbott, *Phys. Rev. Lett.* **119**, 161101 (2017).
2. P. S. Cowperthwaite *et al.*, *Astrophys. J. Lett.* **848**, L17 (2017).
3. N. R. Tanvir *et al.*, *Astrophys. J. Lett.* **848**, L27 (2017).
4. M. M. Kasliwal *et al.*, *Science* **358**, 1559–1565 (2017).
5. M. W. Coughlin *et al.*, *Mon. Not. R. Astron. Soc.* **480**, 3871–3878 (2018).
6. M. R. Drout *et al.*, *Science* **358**, 1570–1574 (2017).
7. D. Kasen, B. Metzger, J. Barnes, E. Quataert, E. Ramirez-Ruiz, *Nature* **551**, 80–84 (2017).
8. D. Watson *et al.*, *Nature* **574**, 497–500 (2019).
9. I. U. Roederer *et al.*, *Astrophys. J. Suppl. Ser.* **260**, 27 (2022).
10. A. P. Ji, A. Frebel, A. Chiti, J. D. Simon, *Nature* **531**, 610–613 (2016).
11. I. U. Roederer, K. Hattori, M. Valluri, *Astron. J.* **156**, 179 (2018).
12. J. J. Cowan *et al.*, *Rev. Mod. Phys.* **93**, 015002 (2021).
13. Materials and methods are available as supplementary materials.
14. F. Montes *et al.*, *Astrophys. J.* **671**, 1685–1695 (2007).
15. Y.-Z. Qian, G. J. Wasserburg, *Astrophys. J.* **687**, 272–286 (2008).
16. S. Wanajo *et al.*, *Astrophys. J. Lett.* **789**, L39 (2014).
17. M. Eichler *et al.*, *Astrophys. J.* **808**, 30 (2015).
18. S. Goriely, G. Martínez Pinedo, *Nucl. Phys. A.* **944**, 158–176 (2015).
19. I. V. Panov, I. Y. Korneev, F.-K. Thielemann, *Astron. Lett.* **34**, 189–197 (2008).
20. T. M. Sprouse *et al.*, *Phys. Rev. C* **101**, 055803 (2020).
21. N. Vassh, M. R. Mumpower, G. C. McLaughlin, T. M. Sprouse, R. Surman, *Astrophys. J.* **896**, 28 (2020).
22. J. M. Miller *et al.*, *Phys. Rev. D* **100**, 023008 (2019).
23. D. Radice *et al.*, *Astrophys. J.* **869**, 130 (2018).
24. M. Reichert, M. Obergaulinger, M. Eichler, M. Á. Aloy, A. Arcones, *Mon. Not. R. Astron. Soc.* **501**, 5733–5745 (2021).
25. J.-F. Lemaître, S. Goriely, A. Bauswein, H.-T. Janka, *Phys. Rev. C* **103**, 025806 (2021).
26. J. Beun, G. C. McLaughlin, R. Surman, W. R. Hix, *Phys. Rev. C Nucl. Phys.* **77**, 035804 (2008).
27. N. Vassh, r-process abundances in neutron star merger dynamical ejecta given different fission yields. Zenodo (2023); https://doi.org/10.5281/zenodo.7127232.

ACKNOWLEDGMENTS

We thank A. Aprahamian, E. Bell, B. Côté, Y. Hirai, G. Mathews, C. Sneden, and M. Wiescher for comments on early versions of the manuscript. **Funding:** We acknowledge support from the US National Science Foundation grants AST 1716251 (to A.F.); AST 1815403 (to I.U.R.); AST 1815767 (to I.U.R.); AST 2205847 (to I.U.R.); OISE-1927130 (IReNA; The International Research Network for Nuclear Astrophysics) (to T.C.B., A.F., and T.T.H.); PHY 14-30152 (JINA-CEE; Joint Institute for Nuclear Astrophysics–Chemical Evolution of the Elements) (to I.U.R., E.M.H., M.R.M., R.S., T.C.B., R.E., and A.F.); and PHY 2020275 (to R.S.). R.S. acknowledges support from the US Department of Energy grants DE-FG02-95-ER40934 and DE-SC0018232. We acknowledge additional support from NASA grants 80NSSC21K0627 (Astrophysics Data Analysis Program; to IUR); HST-GO-15657 (to I.U.R., T.C.B., A.F., and V.M.P.); HST-GO-15951 (to I.U.R., T.C.B., R.E., A.F., T.T.H., and C.M.S.); and HST-HF2-51481.001 (National Hubble Fellowship Program) (to E.M.H.). N.V. acknowledges support from the Natural Sciences and Engineering Research Council of Canada. M.R.M. acknowledges support from Los Alamos National Laboratory's Directed Research and Development program 20200384ER. T.T.H. acknowledges support from grant VR 2021-05556 from the Swedish Research Council. V.M.P. acknowledges support from NOIRLab, which is managed by the Association of Universities for Research in Astronomy under a cooperative agreement with the US National Science Foundation. **Author contributions:** Conceptualization: I.U.R. Formal Analysis: I.U.R. and T.C.B. Methodology: I.U.R., N.V., E.M.H., M.R.M., and R.S. Investigation: I.U.R. and N.V. Visualization: I.U.R., N.V., E.M.H., M.R.M., R.S., J.J.C., and T.C.B. Writing – original draft: I.U.R. and N.V. Writing – review and editing: I.U.R., N.V., E.M.H., M.R.M., R.S., J.J.C., T.C.B., R.E., A.F., T.T.H., V.M.P., and C.M.S. **Competing interests:** The authors declare that they have no competing interests. **Data and materials availability:** Our compilation of stellar abundance data for the 42 stars in our sample is available in data S1. The nucleosynthesis yields (*21*) we used as input for our fission calculations are archived at Zenodo (*27*). Our derived correlations are quantified in table S1, and the empirical *r*-process baseline abundances are listed in tables S2 and S3.

SUPPLEMENTARY MATERIALS

science.org/doi/10.1126/science.adf1341
Materials and Methods
Supplementary Text
Figs. S1 to S6
Tables S1 to S3
References (*28*–*130*)
Data S1

Submitted 30 September 2022; accepted 6 November 2023
10.1126/science.adf1341